Refined geometry and frozen phonons in $KNbO_3$

A. V. Postnikov* and G. Borstel
Department of Physics, University of Osnabrück, D-49069 Osnabrück, Germany

Abstract

Full-potential LMTO calculations for $KNbO_3$ reported up to now provided a reasonable description of off-center equilibrium displacements, including transversal optical Γ phonons. However, when addressing more sensitive phonon properties and the behavior of the ferroelectric instability over the Brillouin zone, the need was realized to achieve a substantially higher level of accuracy.

In order to arrive at ultimately accurate results available with the LMTO method in the local density approximation, the stability of full-potential LMTO predictions for off-center displacements in $KNbO_3$, as depending on the choice of basis and expansion cutoffs, has been thoroughly investigated.

With the calculation setup thus optimized, supercell frozen phonon calculations aimed at the study of the chain-structure instability over the Brillouin zone have been done, and the long-wavelength limit of the LO phonon is discussed.

I. INTRODUCTION

In referring to the nature of the ferroelectric instability in $KNbO_3$, which develops as Nb atoms are displaced from their symmetric positions in the centre of the cubic perovskite cell, it became usual to mention a crossover from displacive to order-disorder type of transition, that gave rise to considerable controversy [1,2,3,4,5]. Indeed, both the temperature dependence of the dielectric constant [6] and the anisotropy of the transverse acoustic and lowest optical phonon branches may be understood in the most natural way in the framework of the displacive model [7]. At the same time, recent stimulated Raman scattering experiments [8,9,10] clearly suggest that separate off-center potential minima for Nb atoms exist, and the hoppings between them can be induced by an appropriate photon pumping. This controversy may be understood in the following way: The displacive scenario supposes that the (in our case Nb) atoms are sitting at, or rather oscillating about, the central symmetric position in the high-temperature paraelectric phase, and this is definitely not the case in $KNbO_3$. In fact Nb atoms are displaced in each individual unit cell all way around through the sequence of phase transitions. But the textbook description of the order-disorder model with Nb atoms statistically distributed over eight [111]-displaced positions is also not true in its implicit assumption that each individual atom has a choice of eight local potential minima around the centre of the perovskite cell. Be it so, the scan

of the potential hypersurface related to the displacement of a *single* individual atom in an otherwise non-polar paraelectric crystal would clearly exhibit these minima. Such scanning, that is difficult to implement experimentally but easy to imitate in a supercell total-energy calculation, shows no traces of off-center minima and no noticeable anharmonic damping of local potential surface related to a *single* atom displacement beyond any uncertainty of calculation [11]. At the same time, precise total-energy calculations for perfectly ordered ferroelectric $KNbO_3$ [12,13,14] routinely reproduce the tendency of Nb atoms to displace *simultaneously* off-center in the [111]-direction, and the Γ-TO frequencies which come out reasonably well in such calculations [12,15,16,17] suggest that the potential hypersurface related to various atomic displacements is described sufficiently well.

The message from this mixed evidence is that the off-center potential minimum for the Nb atom in each individual perovskite cell is determined by the electric field in some vicinity of the cell in question. In other words, the displacement of Nb atoms is correlated, and the ferroelectric instability develops as the softening of particular phonon modes. This statement belongs to the vocabulary of the displacive model. The important difference is that the particular vibration pattern may have finite spatial extent, or correlation length, even at very low temperatures. Another difference is that a particular soft mode may not necessarily freeze down with temperature, but rather remain frozen at all temperatures throughout the ferroelectric transitions. What evolves with temperature is either the statistical mixture, or the dynamical interplay, of different frozen modes, apparently accompanied by a gradual decrease of the correlation length.

With respect to spatially correlated displaced Nb atoms, a guess that they may build chain-like structures has been put forward long ago by Comes *et al.* [18] and since then addressed by new measurements (see, e.g., Ref. [19]). It was not however possible to extract experimentally any information as for the correlation length along the chain, nor to whether there is any correlation between different chains. From the lattice-dynamical point of view, the study of the spatial correlation along the chain has to do with the instability region, i.e. that of the soft-mode freezing, in some vicinity of the Brillouin zone center. Yu and Krakauer [20] mapped the phonon spectrum of cubic $KNbO_3$ over the whole Brillouin zone in an *ab initio* calculation using a linear response approach. Once the general shape of the instability region is known, additional information on the correlation in the atomic displacements, which may as well include the effects beyond the harmonic approximation, may be obtained from supercell calculations. In the present paper, we provide a preliminary attempt of such analysis, based on the use of a fast full-potential linear muffin-tin orbital (LMTO) method.

II. REFINED CALCULATION SETUP FOR THE FULL-POTENTIAL LMTO CALCULATIONS OF $KNbO_3$

Using the fast and accurate full-potential LMTO code by M.Methfessel [21,22] as a tool for *ab initio* total energy calculations, we were able to study earlier in a series of papers [11,13,15,16] different aspects of ferroelectricity in $KNbO_3$, including magnitudes of equilibrium off-center atomic displacements, coupling of the displacements to the (tetragonal) lattice strain, and Γ-TO phonon frequencies in different phases of this compound. Keeping in mind the planned applications to large supercells, we tried to analyze the resources of the

method and of our previously used setup concerning an eventual decrease in the computational demand without substantial loss of accuracy. At the same time, we tried to find a way to improve the description of the O–K bonding, which came out somehow too rigid in our previous calculations. As a result, the coupling of K to the oxygen cage on a ferroelectric transition was overestimated – see the discussion in Ref. [15].

We considered the refinement of our calculation setup along the following guidelines: The choice of the muffin-tin spheres sizes is based on the spatial distribution of the potential over the cell (with the exception of K whose sphere is enlarged in order to include some interstitial space around it) and need not to be changed compared to as discussed in Ref. [13]; the same applies to the kinetic energies of the Hankel function envelopes (-0.01, -1.0 and -2.3 Ry) which provide sufficient variational freedom. As has been discussed at length in Section III of Ref. [13], one possible source of uncertainty in the calculation results is the termination of the spherical harmonic expansions of the charge density in the interstitial region at some value L_{max} (in principle different for each inequivalent atom type). The usual way to control this is to check the convergency of results depending on this parameter. Another option in the adjustment of the calculation setup is the choice of the basis LMTO's. As a reference point representing convergency with respect to both these factors, we considered the calculation with L_{max}=6 on all atoms, and all valence-state basis functions (s, p and d) included in the basis set for each value of the Hankel function energy. The systematic analysis of the trends in the calculated properties (we concentrated mostly on the magnitude of the equilibrium off-center Nb displacement from the cubic phase and the corresponding energy lowering) has then been done in order to find a more economic setup, with respect to L_{max} and the basis choice, that does not result in a noticeably loss of accuracy.

For the K atom with its uncommonly large muffin-tin sphere, we found it preferable to keep L_{max}=6, whereas for Nb and O atoms with much smaller spheres the cutoff L_{max}=4 suffices, as is consistent with the experience of other calculations performed with the code by M.Methfessel. As regards the basis set, we found it necessary to include all $5s$, $4p$ and $4d$ states combined with all three Hankel function tails on the Nb site, i.e. adding p and d states matched with the Hankel function of the lowest tail energy (-2.3 Ry) as compared with the prescription of Ref. [13]. The choice of basis functions related to K and O sites did not need to be changed. Note that the inclusion of the $3d$ states on O sites for at least one (the highest) envelope function energy is essential for describing the very existence of the ferroelectric instability. We checked that the further enhancement of the O basis set using the $3d$ functions matched to other Hankel envelopes does not lead to any substantial changes. On the K site, the basis functions matched with the lowest-lying Hankel envelope may be thrown out whatsoever.

These refinements do not affect the total energy dependence on volume in any noticeable way, nor do they result in substantial changes of the total energy vs. Nb displacement behavior in cubic or tetragonal phases of $KNbO_3$, compared to the results of Refs. [13,15,11]. However, for the orthorhombic phase characterized by much smaller energy differences on displacement and tiny magnitudes of the equilibrium displacements, our present results may be considered as some improvement over those preliminarily reported in Ref. [16].

TABLE I. Positions of atoms in orthorhombic phase of $KNbO_3$ (in terms of lattice parameters) as determined by neutron diffraction measurements, Ref. [23], and optimized in the FP-LMTO total-energy calculation.

	Atom	a	b	c		Δ_{exp}	Δ_{calc}
1	K	0	0	Δ_z		0.0138	0.0314
2	Nb	$\frac{1}{2}$	0	$\frac{1}{2}$			
3	O(I)	0	0	$\frac{1}{2}+\Delta_z$		0.0364	0.0351
4	O(II)	$\frac{1}{2}$	$\frac{1}{4}+\Delta_y$	$\frac{1}{4}+\Delta_z$	Δ_z :	0.0342	0.0353
5	O(II)	$\frac{1}{2}$	$\frac{3}{4}-\Delta_y$	$\frac{1}{4}+\Delta_z$	Δ_y :	-0.0024	-0.0037

III. EQUILIBRIUM STRUCTURE OF THE ORTHORHOBMIC PHASE OF $KNbO_3$ AND Γ-TO PHONONS

With the calculation setup as described above, we performed the total energy-driven optimization of atomic positions in the orthorhombic phase. In the setting used by Hewat [23], the three lattice vectors are a=3.973Å along $\mathbf{x}$=[100] of the cubic aristotype; b=5.695Å along $\mathbf{y}$=[0$\bar{1}$1], and c=5.721Å along $\mathbf{z}$=[011]. The positions of the atoms have been optimized in a four-dimensional parameter space as done earlier in Ref. [16], i.e. keeping the lattice volume and strain constant in agreement with the experimental data. The displacements of atoms from their symmetry positions in terms of corresponding lattice vectors are shown in Table I. As compared with earlier FP-LMTO calculations with a slightly different setup [16], the z-displacement of K was somehow reduced and the z-displacement of both O(I) and O(II) increased, resulting in better agreement with the experimental geometry; the estimate of the small O(II) displacement in the y direction also became more accurate. Of all structure parameters, only our estimate of the K z-displacement still remains beyond the experimental uncertainty as given in Ref. [23].

Based on this refined geometry, we calculated the Γ-TO phonon frequencies as another benchmark for the quality of our description of the total energy hypersurface as a function of atomic displacements. The symmetry coordinates for the displacements from the equilibrium positions in the $Amm2$ space group of orthorhombic $KNbO_3$ are as given in Ref. [16]. Based on a polynomial fit of the total energy hypersurface in terms of symmetry coordinates, we calculated the frequencies of the phonon modes compatible with the B_2 (that including the soft mode) irreducible representation within our new calculation setup. The frequencies and eigenvectors are shown in Table II. As compared to our earlier calculation [16], we obtained somehow better agreement with the experimental frequencies. Moreover, the contribution of the K displacement in the eigenvector of the soft mode decreases, which means that the soft mode represents primarily the vibration of Nb against the oxygen sublattice, with relatively unaffected K in the background. This seems to be in better agreement with the displacement pattern of atoms in the rhombohedral structure that emerges as the B_2 soft mode freezes down, and thus fixes the unaccuracy pointed out in our previous study where the coupling of K to the oxygen octahedra was overestimated (see Fig.1 of Ref. [16]). The calculated frequency of the A_2 mode is 252 cm^{-1}, which is again in somehow better agreement with the experimental estimate of 283 cm^{-1} [24] than 224 cm^{-1} as calculated in Ref. [16].

TABLE II. Calculated Γ-TO frequencies and eigenvectors for the B_2 modes in orthorhombic $KNbO_3$.

Eigenvectors (present work)					ω calc. (cm^{-1})	ω exp. (cm^{-1})
K	Nb	O_1	O_2	O_3		
0.14	−0.62	0.63	0.32	0.32	$169i$	soft
−0.82	0.32	0.47	0.02	0.02	204	195[a]–197[c]
−0.30	−0.05	−0.54	0.56	0.56	607	511[a]–516[c]

[a] Raman spectroscopy; Ref. [24].
[c] Infrared spectroscopy; Ref. [1].

IV. CHAIN STRUCTURES AND OFF-Γ FROZEN PHONONS

A complete mapping of the phonon frequencies over the Brillouin zone of cubic $KNbO_3$ has been done by Yu and Krakauer [20] in an *ab initio* linear response calculation. Straightforward supercell calculations are too time consuming for any dense mapping of this kind, nor are they feasible for an arbitrary **k** point. They may be however useful for going beyond the harmonic approximation for phonons, which is a natural limitation of a linear response approach, and for analyzing the ferroelectric instability in more detail for several selected **k** points. In principle, the continous mapping over the Brillouin zone is as well possible based on a selection of representative supercell calculations for the fitting of the total energy expansion coefficients, as has been proposed by Wei and Chou [25]. This is only a question of the computational effort, but not a principal limitation.

In the present paper, we provide some preliminary results concerning the chain-structure instability in orthorhombic $KNbO_3$. We performed the calculations for the experimental lattice parameters as discussed in Section III, i.e. for the cell volume very close to that used in Ref. [20]. Since the orthorhombic distortion is rather small, one should not expect large differences in what regards the region of ferroelectric instability. We concentrated therefore on the total energy lowering as a function of finite atomic displacements, with the ultimate aim to study the effect of displacement correlations on the anharmonic stabilization of structure. For the construction of supercells and the underlying symmetry analysis, we found the software tools developed by Stokes [26] very useful. When considering the frozen phonon for a **k** point along a [100] or [010] symmetry line in an orthorhombic perovskite structure, the soft mode is mixed among 9 coupled symmetry coordinates, that demands a corresponding fitting of the total energy hypersurface. For preliminary estimates, we considered only [100]-displacement of Nb, that dominate in the soft-mode eigenvector as is known from the single-cell calculations. The displacements of Nb atoms within particular patterns, depending on the given **k** vector, are from their equilibrium positions in the orthorhombic structure as discussed in Section III.

In order to check how the ferroelectric instability varies over the (100) plane in the reciprocal space, we considered the points $Y = [010]$ and $S = [0\frac{1}{2}\frac{1}{2}]$, that come into M and X of the cubic structure in the limit of small orthorhombic distortions. In the direct space, corresponding arrangements are infinite [100] chains of stockpiled primitive cells, with Nb atoms displaced along [100] in half of the chains and in the opposite direction in the other half. With respect to each other, these "up" and "down" chains either pack in the chessboard

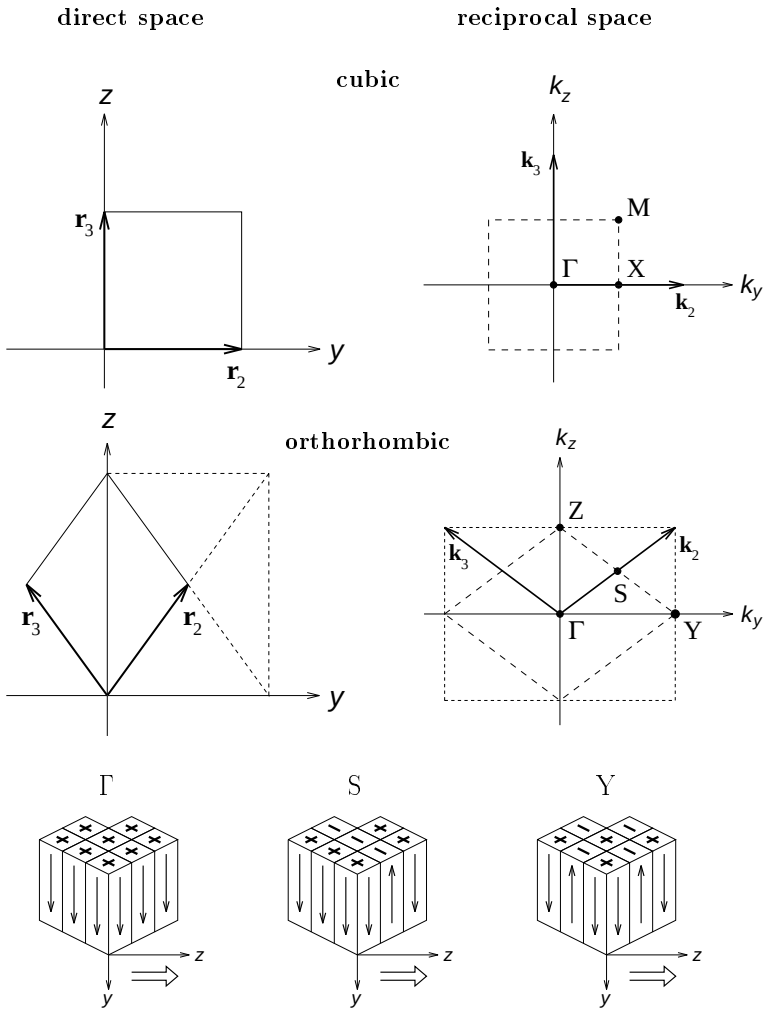

FIG. 1. Relation between cubic and orthorhombic settings in direct and reciprocal space (top), and schematic orientation of dipole moments within chains for supercells corresponding to Γ, S and Y **k**-vectors (bottom). Note that the electric field along chains is on top of the macroscopic field along the z axis.

configuration (Y), or stick to form interchanging planes (S). The relations between cubic and orthorhombic settings and the relevant real-space superstructures are shown in Fig.1.

One can expect from the analysis of Ref. [20] that the force constant related to the soft mode is not changed significantly along the Γ–X–M directions. It follows from our earlier study of different Nb displacement patterns [16] that the force constants corresponding to Γ and Y are indeed very close (see Fig.3, patterns a and b, of Ref. [16]). However, the chessboard confguration of chains turns out to be more stable, allowing larger magnitude of Nb displacements within the chains. The present study supports this conclusion, now with the magnitudes of displacements and the energy gains somehow adjusted with our refined calculation setup, and the data for the S frozen phonon added. The total energy gain as a function of Nb displacements is shown in Fig. 2. As may be intuitively expected, the curve corresponding to the S phonon is the intermediate one between those for Γ and Y, but

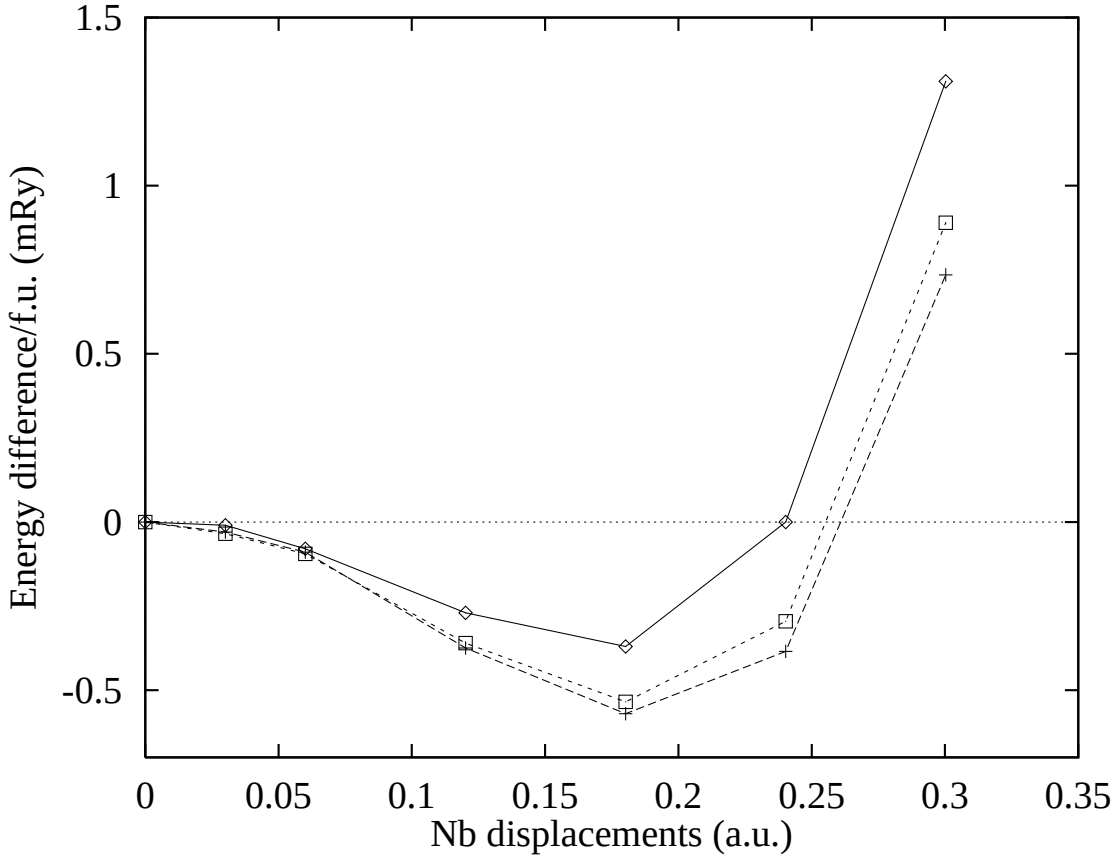

FIG. 2. Total energy difference (per formula unit) as a function of the [100] Nb displacement for the TO Γ, S and Y frozen phonons.

rather close to the latter. This type of mutual arrangement can be easily understood from electrostatic considerations. Electric dipoles, created (on top of the [001] macroscopic field) by additional [100] or [$\bar{1}$00] Nb displacements in individual orthorhombic cells, tend to form chains, but dipoles from different chains, when the latter come closer, have an energy gain if oriented antiparallel. The chessboard configuration realizes the maximal separation between parallel dipoles on a (100) two-dimensional lattice. Due to the anisotropy of the dipole field, the dipole-dipole interaction between chains is much weaker than inside a chain. As a consequence, the ideal chessboard arrangement is not bound to occur at temperatures of the order 300 K ∼1.9 mRy; instead, the chains may be considered as relatively independent (and irregular) in their orientation, as long as the number of "up" and "down" chains remains roughly equal [27].

This consideration effectively sets the correlation length within the (100) plane, i.e. in the direction normal to chains, to one lattice parameter. The analysis of the correlation length along chains demands to go away from the (100) plane in the reciprocal space, e.g., along $M \rightarrow R$ in the cubic setting, and considers the hardening condition of the corresponding transversal phonon mode. Based on a $\omega^2 = 0$ condition for a harmonic frequency at a critical correlation length, Yu and Krakauer [20] set the latter at about 5 lattice spacings. For the orthorhombic lattice, we did the corresponding analysis with a frozen phonon calculation

for several $\mathbf{q}$ points on a $Y \rightarrow T$ line. The values of the force constant related to the [100] displacement of Nb as calculated for several increasingly larger supercells of this type are shown in Fig.3 and connected (as a guideline) by a dashed curve labelled $Y + k_x$. The supercells have the arrangement of chains as is shown in Fig.1 in the (100) plane; the [100] Nb-displacements within the chains are however now varied as $\Delta_x(\mathrm{Nb}) = u\cos(k_x x)$. Each supercell represents therefore a body-centered orthorhombic structure with 2, 4 or 8 formula units per primitive cell; the force constant is the total energy per unit cell twice differentiated in the displacement amplitude u. For $k_x = 0$, the value -65.6 mRy/a.u.^{2} obtained from the double-cell calculation of the Y phonon (as shown in Fig.2) is plotted. The sketches in Fig.3 below show the [100] Nb displacement pattern in the supercells. One can see that the ferroelectric instability develops at $k_x \leq 0.11$, i.e. the critical half-period of the Nb displacement wave that creates a self-supporting instability is between 4 and 5 unit cells. This is in agreement with the estimate done by Yu and Krakauer [20]. For a more accurate analysis however, one should construct and diagonalize the 9×9 dynamicial matrix and search for the condition of a zero eigenvalue to occur.

As another set of examples for off-Γ frozen phonons, we considered several Λ points on a [100] line, that corresponds to the uniform Nb displacement pattern over the (100) plane, but with harmonic variation (represented by increasingly larger supercells) of $\Delta_x(\mathrm{Nb}) \sim \cos(k_x x)$ in the normal direction. The values of the force constant corresponding to this setting are shown in Fig.3 as laying at a solid line labelled $\Gamma + k_x$. Since in this case the phonon mode in question is longitudinal, it should not be expected to get soft even at small values of k_x. The problem of interest in this case is the extrapolation of the force constants towards those for the Γ-LO phonon. The conventional way of treating the Γ-LO phonons is via correcting the dynamical matrix to Born effective charges (see, e.g., [17,28]). Although physically transparent, this method incorporates parameters which have to be extracted from different schemes. Born effective charges are usually fitted from calculations of the finite bulk polarization; the optical macroscopic dielectric function $\varepsilon_\infty(\mathbf{q}, \omega)$ is either extrapolated to $\omega = 0$ from experimental data (Zhong *et al.* cite the value ε_∞=4.69 for $KNbO_3$ [17]), or obtained from a linear response calculation, with a typically overestimated, due to the local density approximation, value (Yu and Krakauer report ε_∞=6.34 [20]). The supercell calculation for the LO phonons, on the contrary, involves only the total energy of the ground state (in principle, without any limitation as regards the anharmonicity), and the effects of long-range polarization and dielectric response are already implicitly included. Taking into account that the force constants should be symmetric with respect to $k_x \rightarrow -k_x$, we extrapolated the force constant related to the [100] Nb displacement in the Γ-LO mode to be 177.2 mRy/a.u.^{2} (see Fig.3). The corresponding force constant in the Γ-TO mode (as extracted from a single-cell calculation; see Fig.2) is -52.3 mRy/a.u.^{2}. Based on the relation between LO and TO force constants (see Ref. [29], or the relevant formulas (2) and (3) in Ref. [17]), we arrive at the following relation between the xx-component of the Nb dynamic effective charge Z^*_{Nb} and ε_∞: $(Z^*_{Nb})^2/\varepsilon_\infty = 3.94$. For the two above cited choices of ε_∞, this leads to an estimate of the relevant Born effective charge between 4.3 (ε_∞=4.69) and 5.0 (ε_∞=6.34). One should note that the Nb-related effective charge tensor is no more diagonal in the orthorhombic structure, and we make no estimates for other elements of it than Z^*_{xx} at the moment. Generally, the value of the xx element in the orthorhombic phase may be expected to be smaller than 9.13 [28] to 9.37 [20] as calculated for the cubic perovskite

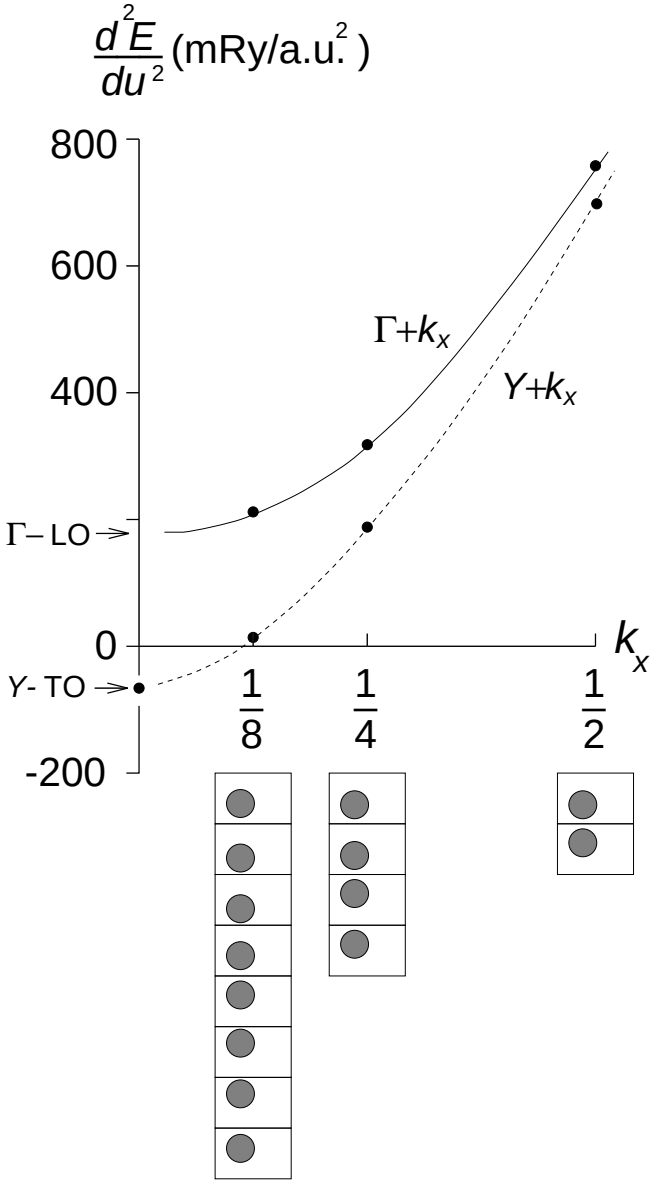

FIG. 3. Force constant of the [100] Nb displacement for TO $[0\,1\,k_x]$ (dots on a dashed line) and LO $[0\,0\,k_x]$ (dots on a solid line) phonons as determined from supercell calculations. The supercells used and corresponding Nb displacement patterns are shown below.

structure by different methods, because the off-center displacement of Nb from the center of a cubic perovskite cell to its position in the orthorhombic cell (along [001], in the present setting) was already accompanied by some charge transfer that reduces the polarizability of the Nb–O bonds in perpendicular directions. Moreover, the [100] displacement of Nb in the orthorhombic phase is not exactly toward an oxygen atom, as it was the case in the cubic structure.

V. CONCLUSION

Based on our previous experience in total-energy calculations with the full-potential LMTO code by M. Methfessel and on the systematic study of the effects of basis choice and the spherical harmonic cutoffs, we attempted to achieve the highest degree of accuracy, attainable with the present status of the code, in the description of microscopic structure of ferroelectric $KNbO_3$ in the room-temperature orthorhombic phase.

This resulted in somehow more accurate, as compared to our previous data, description of the equilibrium geometry, i.e. of optimized off-center displacements of atoms, with the lattice parameters and the orthorhombic strain kept fixed. The Γ-TO phonon frequencies calculated for the B_2 mode are on average in the same degree of agreement with experimental data as in earlier calculations, and the frequency for the A_2 mode has improved. Making use of the computational efficiency of the code, we attempted to model several more complicated frozen phonon patterns in the supercell calculations with up to 40 atoms, aiming at the study of the chain instability and of long-wavelength LO modes. The correlation length for the onset of the ferroelectric instability is estimated to be between 4 and 5 lattice constants in the [100] direction, i.e. along the chains of displaced Nb atoms, which is consistent with the results of a linear response calculation by Yu and Krakauer. The correlations between different chains (in the perpendicular direction) are found to be unimportant for the onset of the ferroelectric instability, but they stabilize the direction of macroscopic polarization compatible with the orthorhombic symmetry, as long as the orthorhombic lattice strain is fixed.

The comparison of force constants, as obtained directly for the Γ-TO mode and extrapolated to $\mathbf{k} \to 0$ from supercell calculations for a LO mode, makes it possible to exploit the relation between Born effective charges and the optical dielectric constant as a tool to estimate whichever of these properties is unknown for the system in question.

ACKNOWLEDGMENTS

The authors are grateful to M. Methfessel for his assistance and advise in using his full-potential LMTO code, and to H. Stokes for providing the symmetry-analysis software. Financial support of the Deutsche Forschungsgemeinschaft (SFB 225) is gratefully acknowledged.

REFERENCES

* Electronic address: apostnik@physik.uni-osnabrueck.de

[1] M. D. Fontana, G. Métrat, J. L. Servoin, and F. Gervais, *J. Phys. C*, **17**, 483 (1984).
[2] M. D. Fontana, A. Ridah, G. E. Kugel, and C. Carabatos-Nedelec, *J. Phys. C*, **21**, 5853 (1988).
[3] J. P. Sokoloff, L. L. Chase, and D. Rytz, *Phys. Rev. B*, **38**, 597 (1988).
[4] M. D. Fontana, G. E. Kugel, and C. Carabatos-Nedelec, *Phys. Rev. B*, **40**, 786 (1989).
[5] J. P. Sokoloff, L. L. Chase, and D. Rytz, *Phys. Rev. B*, **40**, 788 (1989).
[6] F. Jona and G. Shirane, "Ferroelectric Crystals," (Pergamon, New York, 1962).
[7] M. D. Fontana, G. E. Kugel, G. Metrat, and C. Carabatos, *Phys. Status Solidi (b)*, **103**, 211 (1981).
[8] T. P. Dougherty, G. P. Wiederrecht, K. A. Nelson, M. H. Garret, H. P. Jensen, and C. Warde, *Science*, **258**, 770 (1992).
[9] T. P. Dougherty, G. P. Wiederrecht, and K. A. Nelson, *Ferroelectrics*, **164**, 253 (1995).
[10] T. P. Dougherty, G. P. Wiederrecht, K. A. Nelson, M. H. Garrett, H. P. Jenssen, and C. Warde, *Phys. Rev. B*, **50**, 8996 (1994).
[11] A. V. Postnikov, T. Neumann, and G. Borstel, *Ferroelectrics*, **164**, 101 (1995).
[12] D. J. Singh and L. L. Boyer, *Ferroelectrics*, **136**, 95 (1992).
[13] A. V. Postnikov, T. Neumann, G. Borstel and M. Methfessel, *Phys. Rev. B*, **48**, 5910 (1993).
[14] R. D. King-Smith and D. Vanderbilt, *Phys. Rev. B*, **49**, 5828 (1994).
[15] A. V. Postnikov, T. Neumann, and G. Borstel, *Phys. Rev. B*, **50**, 758 (1994).
[16] A. V. Postnikov and G. Borstel, *Phys. Rev. B*, **50**, 16403 (1994).
[17] W. Zhong, R. D. King-Smith, and D. Vanderbilt, *Phys. Rev. Lett.*, **72**, 3618 (1994).
[18] R. Comes, M. Lambert, and A. Guinier, *Solid State Commun.*, **6**, 715 (1968).
[19] M. Holma, N. Takesue, and H. Chen, *Ferroelectrics*, **164**, 237 (1995).
[20] Rici Yu and H. Krakauer, *Phys. Rev. Lett.*, **74**, 4067 (1995).
[21] M. Methfessel, *Phys. Rev. B*, **38**, 1537 (1988).
[22] M. Methfessel, C. O. Rodriguez, and O. K. Andersen, *Phys. Rev. B*, **40**, 2009 (1989).
[23] A. W. Hewat, *J. Phys. C*, **6**, 2559 (1973).
[24] D. G. Bozinis and J. P. Hurrell, *Phys. Rev. B*, **13**, 3109 (1976).
[25] S. Wei and M. Y. Chou, *Phys. Rev. Lett.*, **69**, 2799 (1992).
[26] H. T. Stokes, *Ferroelectrics*, **164**, 183 (1995).
[27] Obviously enough, the rhombohedral phase with all chains, say, in "up" configuration must have lower total energy as a result of optimization in volume along with *all* coordinate and strain variables. The structure compatible with the Y phonon comes out as the most stable one in our calculation under the constraint of fixed orthorhombic lattice parameters.
[28] R. Resta, M. Posternak, and A. Baldereschi, *Phys. Rev. Lett.*, **70**, 1010 (1993).
[29] R. M. Pick, M. H. Cohen, and R. M. Martin, *Phys. Rev. B*, **1**, 910 (1970).